Heliyon 10 (2024) e23402

Contents lists available at ScienceDirect

Heliyon

journal homepage: www.cell.com/heliyon

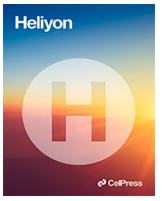

Huoxin pill protects verapamil-induced zebrafish heart failure through inhibition of oxidative stress-triggered inflammation and apoptosis

Xianmei Li [a,1], Laifeng Zeng [a,1], Zhixin Qu [b], Fenghua Zhang [b,*]

[a] *Fujian Key Laboratory of Integrative Medicine on Geriatrics, Academy of Integrative Medicine, Fujian University of Traditional Chinese Medicine, Fuzhou, 350122, PR China*

[b] *Key Laboratory of Gastrointestinal Cancer (Ministry of Education), School of Basic Medical Sciences, Fujian Medical University, Fuzhou, 350122, PR China*

ARTICLE INFO

Keywords:
Huoxin pills
Heart failure
Zebrafish
Oxidative stress
Inflammation
Apoptosis

ABSTRACT

Heart failure (HF) is a major and growing public health concern. Although advances in medical and surgical therapies have been achieved over the last decades, there is still no firmly evidence-based treatment with many traditional Chinese medicines (TCMs) for HF. Huoxin Pill (HXP), a TCM, has been widely used to treat patients with coronary heart disease and angina pectoris. However, the underlying molecular mechanism is poorly understood. In this study, using a verapamil-induced zebrafish HF model, we validated the efficacy and revealed the underlying mechanism of HXP in the treatment of HF. Zebrafish embryos were pretreated with different concentrations of HXP followed by verapamil administration, and we found that HXP significantly improved cardiac function in HF zebrafish, such as by effectively alleviating venous congestion and increasing heart rates. Mechanistically, HXP evidently inhibited verapamil-induced ROS and H_2O_2 production and upregulated CAT activity in HF zebrafish. Moreover, transgenic lines *Tg(mpx:EGFP)* and *Tg(nfkb:EGFP)* were administered for inflammation evaluation, and we found that neutrophil infiltration in HF zebrafish hearts and the activated NF-kB level could be reduced by HXP. Furthermore, HXP significantly downregulated the level of cell apoptosis in HF zebrafish hearts, as assessed by AO staining. Molecularly, RT−qPCR results showed that pretreatment with HXP upregulated antioxidant-related genes such as *gpx-1a* and *gss* and downregulated the expression of the stress-related gene *hsp70*, proinflammatory genes such as *tnf-α*, *il-6* and *lck*, and apoptosis-related indicators such as *apaf1*, *puma* and *caspase9*. In conclusion, HXP exerts a protective effect on verapamil-induced zebrafish HF through inhibition of oxidative stress-triggered inflammation and apoptosis.

1. Introduction

Heart failure (HF) is a complicated clinical disease characterized by cardiac enlargement, severe venous congestion, slowing heartbeat and reduced ability of the heart to pump and/or fill blood. Since it affects at least 26 million people worldwide, HF has been

* Corresponding author.
E-mail address: zfh0606@fjmu.edu.cn (F. Zhang).
[1] These authors contributed equally to this work.

https://doi.org/10.1016/j.heliyon.2023.e23402
Received 19 August 2023; Received in revised form 27 November 2023; Accepted 4 December 2023
Available online 9 December 2023

defined as a global pandemic with an increasing prevalence [1]. Although the medications we can use to treat HF are diversified with deeper insight in this field, the prognosis remains poor, and the mortality is still high [2–4]. In recent years, the application of traditional Chinese medicine (TCM) has gradually become universally accepted for HF treatment, such as the Danqi pill [5], Yiqifumai pill [6] and Huoxin pill (HXP) [7]. However, the mechanisms involved are still at an initial stage. Therefore, the prevention and treatment of HF using TCMs urgently needs more fundamental studies.

HXP is a TCM formula that has achieved good curative effects in clinical settings [8], and has been widely used for the treatment of coronary heart disease and chronic heart failure in Asia for decades [8,9]. It is composed of ten ingredients, including *Ganoderma lucidum* (Leyss. ex Fr.) Karst., *Panax ginseng* C. A. Mey., *Aconitum carmichaeli* Debx., *Margaritifera*, *Ursi fellis pulvis*, *Carthamus tinctorius* L., *Bufonis venenum*, *Moschus*, *Bovis calculus artifactus* and *Borneolum syntheticum,* and they were mixed at a ratio of 33:30:15:4:4:3:3:2:2:2. Numerous components in HXP have been proven to exert antioxidative effects that may protect against heart injury, such as *Ganoderma lucidum* and *ginsenosides* from *Panax giseng* [10,11]. However, research on the mechanism by which HXP protects against cardiovascular diseases, particularly HF, is limited.

Mammalian models have been used extensively to study the mechanisms of HF. However, in recent years, based on advantages such as small size, low cost, ease of use and convenient imaging, the zebrafish model has offered inspiring possibilities for drug discovery, as it possesses high levels of genetic and organ functional similarities with humans [12–14]. In fact, most of the specialized cell types, structures, contributing cell types and vital signaling pathways are also conserved between zebrafish and mammalian hearts despite the simplicity of the zebrafish heart [15–17]. Thus, zebrafish have become a highly suitable model to decipher human cardiac disease and screen relevant drugs at the preclinical stage [18,19]. For example, a verapamil-induced zebrafish HF model has been reported as an alternative and convenient tool for rapid in vivo efficacy assessment and HF therapeutic drug screening [20]. As the development of zebrafish heart almost completed at the time point of 48 hpf [21], many researchers utilized 48 hpf zebrafish to build the HF model [22–24].

Oxidative stress plays a critical role in the pathogenesis of HF [25,26]. A variety of clinical and experimental studies have shown that increased oxidative stress induced by abnormal production of reactive oxygen species (ROS) in the myocardium is closely intertwined with inflammation and that one amplifies the other [27–29]. Oxidative stress is strongly associated with the expression of various inflammatory transcription factors, such as nuclear factor-kB (NF-kB) that modulates proteolytic pathways and promotes inflammation [30]. Activation of NF-κB by various factors plays an important role in the inflammatory response and cell apoptosis [31, 32]. It has been reported that myocardial levels of NF-κB were increased in patients with advanced heart failure, and NF-kB-mediated signaling may have a central role in orchestrating the molecular processes that contribute to heart failure [33,34].

It is worth noting that, to evaluate the drug efficacy on HF zebrafish, the distinction between the potential general toxic response elicited by the drugs and their specific effects on heart development and function should be clarified. General toxic response refers to non-specific toxic effects that a drug may have on various tissues or organs, including the heart. These responses can manifest as overall damage to tissue architecture, cell death, or disruption of normal physiological processes. On the other hand, specific effects on zebrafish heart development and function are observed when a drug specifically targets molecular pathways relevant to cardiac development or impacts cardiac function without causing widespread toxicity. These effects are more likely to occur at lower concentrations of the drug and involve mechanisms that specifically influence heart-related processes, such as modulation of key signaling pathways involved in heart development or function. This distinction is essential for accurately interpreting the results and understanding the mechanisms through which the drugs act on.

Our current study utilized a verapamil-induced zebrafish HF model to examine the protective role of HXP and verify the potential underlying mechanism involved. Here, we show that HXP alleviated verapamil-induced HF in zebrafish by clearing ROS, suppressing the inflammatory response and inhibiting cell apoptosis in the heart. This research may facilitate the clinical application of HXP for many other cardiovascular diseases.

2. Materials and methods

2.1. Experimental animals: zebrafish (Danio rerio)

Adult zebrafish were housed in a light and temperature controlled aquaculture facility with a standard 14 h light/10 h dark photoperiod and fed brine shrimp twice daily and dry flakes (LARVAQUA，China) once a day. Four to five pairs of zebrafish were set up for natural mating every time. Embryos were maintained at 28.5 °C in 0.3 × Danieaus' buffer (NaCl 20.34 g, KCl 0.313 g, $MgSo_4 \bullet 7H_2O$ 0.592 g, Ca (NO_3) $_2 \bullet 4H_2O$ 0.850 g, HEPES 7.12 g, H_2O 20 L). All animal research conformed to the Guidelines for the Care and Use of Laboratory Animals published by Fujian University of Traditional Chinese Medicine. The *Tg(mpx:EGFP)*, *Tg(myl7:EGFP)* and wild type AB strains of zebrafish were purchased from the China Zebrafish Resources Center (CZRC, Wuhan). Among them, transgenic lines *Tg(mpx:EGFP)* and *Tg(myl7:EGFP)* labeled neutrophils and myocardial cells respectively with green fluorescence protein. The *Tg(nkfb:EGFP)* transgenic line, which can show the expression level of NF-kB protein with green fluorescence, was a gift from Fuzhou Bioservice Biotechnology Co., Ltd. The stages of embryonic development refer to a previous paper [35].

2.2. Main experimental reagents and equipment

HXP was purchased from Guangzhou Yuekang Biopharmaceutical company (lot#: 21050101); verapamil was purchased from Solarbio company (CAS#: 52-53-9, chemical formula: $C_{27}H_{38}N_2O_2$, concentration: 100 mM in DMSO); the NovoScript®Plus All-in-one 1st Strand cDNA Synthesis SuperMix (gDNA Purge) (Cat. No.: E047) and NovoStart®SYBR qPCR SuperMix Plus (Cat. No.: E096) were

purchased from Nearshore Protein Technology Company. The AO Dyeing kit was from Maclean Company (lot#: A860545); the DCFH-DA fluorescent probe was purchased from Shanghai Yuanye Biotechnology Company (lot#: J30GS153026); the Hydrogen Peroxide Assay Kit (S0038) and Catalase Assay Kit (S0051) were purchased from Beyotime Biotechnology; the THZ-100 incubator was purchased from Shanghai Yiheng Company; and the SMZ800 N stereoscopic fluorescence microscope was purchased from Nikon Company.

2.3. Preparation of HXP extract and composition analysis

HXP was ground or pounded into a fine powder that passed through a sieve with a nominal mesh aperture of 180 μm. The dried powder was dissolved in DMSO to a concentration of 4 mg/mL. It was filtered with a 0.22 μm filter and stored at −20 °C for further use.

We investigated the chemical composition of HXP by ultra-high pressure liquid phase-time-of-flight high-resolution mass spectrometry. 300 mg HXP powder were added to 3 mL 50 % methanol aqueous solution. After mixing, the mixture was sonicated at 45 °C for 1 h, and then allowed to stand for 5 min. The supernatant was centrifuged for 10 min at 13,000 rpm/min. The supernatant was passed through a 0.22-μm filter, and then the filtrate was subjected to chromatography using a Agilent 1290 (UL61010A-1) system and Agilent 6550 QTOF ultra-high resolution mass spectrometry system. The extraction solution was separated on a waters BEH C18 column (1.7 μm, 2.1*100 mm) with gradient elution. Aqueous 0.1 % formic acid solution (A) and methanol (B) were used as mobile phase and the gradient elution procedure was as follows: 0 min, A:B = 90:10; 5 min, A:B = 90:10; 20 min, A:B = 10:90; 30 min, A:B = 10:90; 33 min, A:B = 90:10; 35 min, A:B = 90:10. The sample volume was 5 μL and the flow rate was 0.3 mL/min.

Total ion chromatogram of the extract of HXP was shown in Fig. S1 and a total of 682 compounds from the HXP constituents have been identified and listed in Table S1.

2.4. Establishment of zebrafish HF model

Zebrafish at 52 hpf were selected as the beginning of the verapamil treatment stage, and the HF model was established [22,23]. Four to five pairs of zebrafish were set up for natural mating every time. 50 embryos from each pairs were collected randomly and mixed together and then cultured in a 90 cm dish with 0.3 × Danieaus' buffer at 28.5 °C. Embryos were randomly divided into a 6-well plate the previous day, 30 embryos per well. Zebrafish embryos were divided into five groups and treated with different concentrations of verapamil (50, 100, 200, 400 μM) and 0.1 % DMSO as vehicle controls for 30 min at 52 hpf. 30 embryos in each group were observed and photographed under a microscope. According to the area of venous congestion and pericardial edema, we classified zebrafish embryos into three phenotypes: normal, moderate, and severe. The ratio of normal, mild and severe phenotypes of venous congestion and pericardial edema as well as the heart rate of zebrafish were calculated to determine the optimal concentration of verapamil for modeling as 100 μM. The results are representative of three independent experiments.

2.5. Treatment with HXP in the zebrafish HF model

HXP safe concentration screen: The 48 hpf zebrafish embroyos were divided into nine groups according to the concentration of HXP (0、5、10、20、40、80、160、320、640 μg/mL), and treated with different concentrations of HXP for 4 h at 48 hpf, there were 30 embryos in each group and each group of zebrafish was observed and photographed under a microscope. The camptocormia ratio, heart rate and fraction shortening of zebrafish were calculated to determine the no observed adverse effect level (NOAEL) of HXP at 20 μg/mL. Thus, 5, 10 and 20 μg/mL were selected as low, medium and high concentrations of HXP for subsequent experiments.

Treatment with HXP in the zebrafish HF model: 48 hpf zebrafish were pretreated with low, medium and high concentrations of HXP for 4 h followed by 100 μM verapamil treatment for 30 min. All the subsequent experiment were conducted with 52.5 hpf embryos after verapamil treatment and the group settings are as follows: blank control group (zebrafish treated with 0.1 % DMSO were used as vehicle controls) , verapamil (100 μM) group, verapamil + HXP-L (5 μg/mL) group, verapamil + HXP-M (10 μg/mL) group and verapamil + HXP-H (20 μg/mL) group. Images and videos (10 s) of the diastolic and systolic stages of the beating zebrafish hearts were obtained by stereomicroscopy, and the cardiac data were measured by ImageJ software based on the images and videos [36]. Qualitative and quantitative results of area measurements of the pericardial sac and venous congestion, ejection fraction, fraction shortening, heart rate and cardiac stroke volume were used to assess the preventive effect of HXP. The results are representative of three independent experiments.

2.6. Statistical formula for cardiac function data

Zebrafish larvae were photographed, cardiac videos were recorded for 15 s under a fluoroscopic microscope, and cardiac data were measured using ImageJ software. The area of venous congestion and pericardial edema was measured, venous congestion improvement rate (%) = (Verapamil group - HXP group)/(Verapamil group - control group) *100 %, pericardial edema improvement rate (%) = (Verapamil group - HXP group)/(Verapamil group - control group) *100 %. Based on the pictures corresponding to the end diastolic and end systolic ventricles from the video file, we measured the major axis (a) and short axis (b) of the ventricle, ventricular volume (V) =(3/4)*π (a/2)* (b/2)2, cardiac output (CO) = ventricular volume(V) * heart rate, the difference between the area of ventricular diastolic and systolic periods (Ad-As) = the area of ventricular diastolic periods (Ad) - the area of ventricular systolic periods (As), Cardiac volume (CV) = ventricular end diastolic volume(Vd)ventricular end systolic volume(Vs), ejection fraction (EF) = CV/Vd, Fraction shortening (FS) = [(ventricular enddiastolic diameter (Dd)) - (ventricular end systolic diameter (Ds))]/Dd; Heart rate

statistics: (10 s) heart rate *6 = (1 min) heart rate.

2.7. Cell apoptosis detection

Acridine orange (AO) was used to detect apoptotic cells in zebrafish larvae. AO dye solution was added to each group at a concentration of 5 μg/mL, and the larvae were incubated at 28.5 $^{\circ}$C for 20 min and washed with 0.3 × Danieaus' buffer twice for 3 min each time. Zebrafish larvae were observed and photographed under a fluorescence microscope. ImageJ software was used to calculate the fluorescence intensity of each group based on the pictures. The results are representative of three independent experiments.

2.8. ROS detection

We utilized DCFH-DA to detect ROS levels in zebrafish larvae. DCFH-DA fluorescent probe solution was added to each group at a concentration of 20 μg/mL. Then, the zebrafish larvae were incubated at 28.5 °C for 30 min and washed with 0.3 × Danieaus' buffer twice for 3 min each time. Zebrafish larvae were observed and photographed under a fluorescence microscope. ImageJ software was used to calculate the fluorescence intensity of each group based on the pictures. The results are representative of three independent experiments.

2.9. Hydrogen peroxide and catalase assay

20 zebrafish larvae each group were collected and rinsed in 1 × PBS (0.01 M) three times. Then, 100 μL RIPA buffer was added, and the embryos were homogenized using a high speed electric homogenizer (Tissuelyser-24, Shanghai Jingxin Industrial Development Co., Ltd.). After centrifugation at 12000×*g* for 3–5 min at 4 °C, the supernatant was collected, and the H_2O_2 content and CAT level were measured according to the manufacturer's instructions. The results are representative of three independent experiments.

2.10. Detecting the number of neutrophils

Adult transgenic zebrafish *Tg(mpx:EGFP)* with green fluorescence-labeled neutrophils were mated. Embryos were collected, and normally developed embryos were selected, placed in 0.3 × Danieaus' buffer and incubated to 48 hpf in a 28.5 °C. incubator. Zebrafish larvae were observed and photographed under a fluorescence microscope, and the number of neutrophils in each group was calculated using ImageJ software. The results are representative of three independent experiments.

2.11. Detecting the NF-kB positive embryos

Adult *Tg(nfkb:EGFP)* transgenic zebrafish were in-crossed. Embryos were collected, and normally developed embryos were selected, placed in 0.3 × Danieaus' buffer and incubated to 48 hpf in a 28.5 °C incubator. 20 zebrafish larvae were observed and photographed under a fluorescence microscope, embryos with NF-kB positive signals were calculated and the fluorescence area of NF-kB positive embryos in each group was calculated using ImageJ software. The results are representative of three independent experiments.

2.12. Real-time PCR assay

10 zebrafish larvae in each group were collected and pooled together to extract RNA (whole larvae) using TRIzol reagent, and the larvae were homogenized using a high speed electric homogenizer (Tissuelyser-24, Shanghai Jingxin Industrial Development Co., Ltd.). Total RNA was reverse transcribed to cDNA using a reverse transcription kit according to the manufacturer's instructions. Real-time quantitative PCR was performed with SYBR-Green master mix in 96-well optical plates by using a QuantStudio 6 Flex Real-Time PCR System (Thermo Fisher Scientific). As a housekeeping gene, *ef1α* expression is not altered by treatment and it was used to normalize our genes expression level. *gpx-1a*, *gss* and *nrf2* are antioxidant related genes, *nfkb1*, *tnf-α*, *il-6* and *lck* were inflammatory related factors, *nkx2.5*, *tbx5*, *gata5* and *hand2* were key transcription factors related to zebrafish heart functions. Primer sequences are listed in Table S2. The results are representative of three independent experiments.

2.13. Data availability statement

Strains and plasmid pTol2(nfkb: egfp-UTRSV40) are available upon request. The authors affirm that all data necessary for confirming the conclusions of the article are present within the article, figures, and tables.

2.14. Statistical analysis

All statistical analyses were performed using GraphPad Prism 8.0 (United states). Data are shown as the mean ± standard error (SEM). All the data were tested for homogeneity of variance and normality, and the experimental data were in accordance with normal distribution. One-way ANOVA, followed by Dunnett's *t*-test was used to analyze the difference among groups. $p < 0.05$ was considered statistically significant. # or *: $p < 0.05$; ## or**: $p < 0.01$; ### or ***: $p < 0.001$.

3. Results

3.1. Determination of NOAEL in HXP-treated zebrafish embryos

Zebrafish embryos at 48 hpf were treated with a series of concentrations of HXP for 4 h, and the phenotypes of zebrafish embryos were classified as normal, moderate and severe according to the degree of camptocormia (Fig. 1A). The statistics show that all of the embryos were normal when treated with HXP at concentrations of 20 μg/mL and below. However, when the concentration reached 40 μg/mL, approximately 18.3 % of zebrafish embryos showed moderate phenotypes, and the ratio and degree of camptocormia increased with increasing HXP concentration (Fig. 1B). Additionally, the heart rate of zebrafish embryos treated with HXP at concentrations of 40 μg/mL and below showed no significant change compared to that of the control group ($P > 0.05$), while there was a dose-dependent reduction in heart rate when the concentration exceeded 80 μg/mL ($p < 0.01$) (Fig. 1C). Furthermore, the fractional shortening of the hearts of the embryos showed no obvious difference, but there was a downward trend when the concentration was 10–160 μg/mL (Fig. 1D). The above data suggested that the NOAEL of HXP was 20 μg/mL in 48 hpf zebrafish embryos, and it will not cause significant damage to cardiac function. Therefore, 5 μg/mL, 10 μg/mL and 20 μg/mL HXP were selected as the low, medium and high concentrations to investigate the dose effect relationship between HXP and HF.

3.2. Establishment of the HF model in zebrafish embryos

The 52 hpf zebrafish embryos were treated with verapamil at different concentrations for 30 min. Venous congestion and pericardial cysts of zebrafish embryos were observed, and the phenotypes were classified as normal, moderate and severe, according to the area of venous congestion and pericardial cysts (Fig. 2A and B). According to the statistics of zebrafish phenotypic proportions, 50 μM verapamil resulted in a 20 % moderate phenotype; 100 μM resulted in a 25 % moderate phenotype and 75 % severe phenotype; 200 μM resulted in a 13 % moderate phenotype and 87 % severe phenotype; and 400 μM resulted in a 100 % severe phenotype (Fig. 2C). In addition, the heart rate was calculated, and we found that 50 μM verapamil decreased the heart rate compared with the control group,

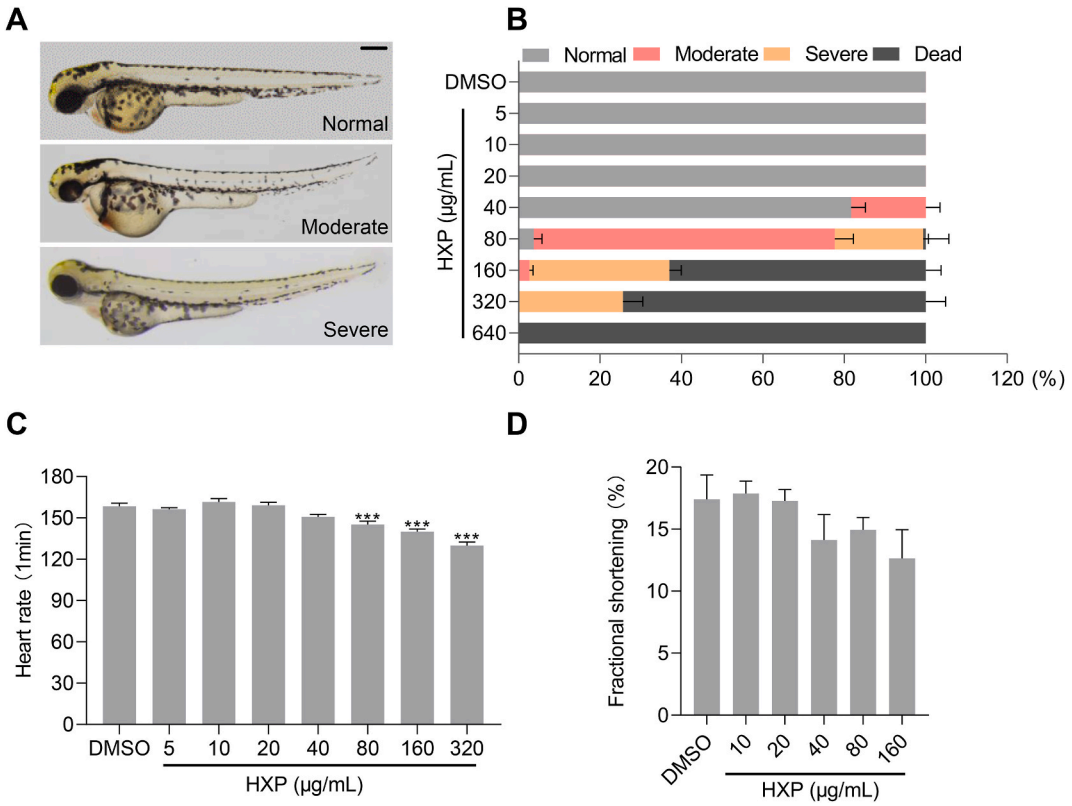

Fig. 1. Effects of HXP on the phenotype and cardiac function of zebrafish embryos **A.** Zebrafish embryos at 48 hpf were exposed to various doses of HXP (0–640 μg/mL) for 4 h. The phenotypes were classified as normal, moderate and severe, scale bar = 200 μm. **B.** Statistics of phenotypic proportions of zebrafish embryos exposed to different doses of HXP (0–640 μg/mL) for 4 h, n = 30, the experiment was replicated three times. **C.** Statistics of the heart rate of zebrafish embryos exposed to different doses of HXP (0–320 μg/mL) for 4 h, n = 30, compared with those of the 0 μg/mL treated group. **D.** Statistics of heart fractional shortening of zebrafish embryos exposed to different doses of HXP (0–160 μg/mL) for 4 h, n = 10, compared with those of the 0 μg/mL treated group (DMSO group).

and 100, 200 and 400 μM verapamil significantly decreased the heart rate in a dose-dependent manner ($P < 0.001$) (Fig. 2D). According to the analysis of the above data, 100 μM verapamil could induce significantly decreased heart rate ($P < 0.001$) and 100 % venous congestion and pericardial cyst (25 % moderate and 75 % severe) in zebrafish embryos. The decreased heart rate and the change in heart morphology suggested cardiac failure. Therefore, 100 μM verapamil was chosen for the establishment of the zebrafish HF model.

3.3. *Protective effect of HXP pretreatment on verapamil-induced HF in zebrafish*

Zebrafish embryos were pretreated with low, medium and high concentrations of HXP for 4 h and then treated with 100 μM verapamil for 30 min. Phenotypic analysis and statistics showed that HXP could relieve the severity of venous congestion and pericardial cysts in zebrafish embryos induced by verapamil (Fig. 3A). It was shown that, in verapamil group, severe phenotype occupied 72 %, moderate phenotype occupied 28 %; in Ver + HXP-L group, severe phenotype occupied 61 %, moderate phenotype occupied 35 %, and normal phenotype occupied 4 %; in Ver + HXP-M group, severe phenotype occupied 46 %, moderate phenotype occupied 45 %, and normal phenotype occupied 9 %; in Ver + HXP-H group, severe phenotype occupied 49 %, moderate phenotype occupied 34 %, and normal phenotype occupied 17 % (Fig. 3B). Quantitative statistics on venous congestion and pericardial cyst area of zebrafish embryos indicated that HXP could reduce the area of venous congestion (Fig. 3C) and pericardial cyst (Fig. 3D) in zebrafish embryos induced by verapamil administration in a dose-dependent manner.

Transgenic zebrafish *Tg(myl7:EGFP)* labeling hearts with green fluorescent protein were treated with drugs as mentioned above and photographed with a fluorescence microscope. Compared with the control group, the heart morphology of zebrafish in the verapamil group was dilated, and the difference between ventricular diastolic and systolic areas was markedly reduced. However, in the Ver + HXP-L, Ver + HXP-M and Ver + HXP-H groups, the embryos showed improved cardiac morphology and recovery of the reduced difference in ventricular diastolic and systolic area (Fig. 3E and F). Moreover, quantitative statistics showed that the heart rate, ejection

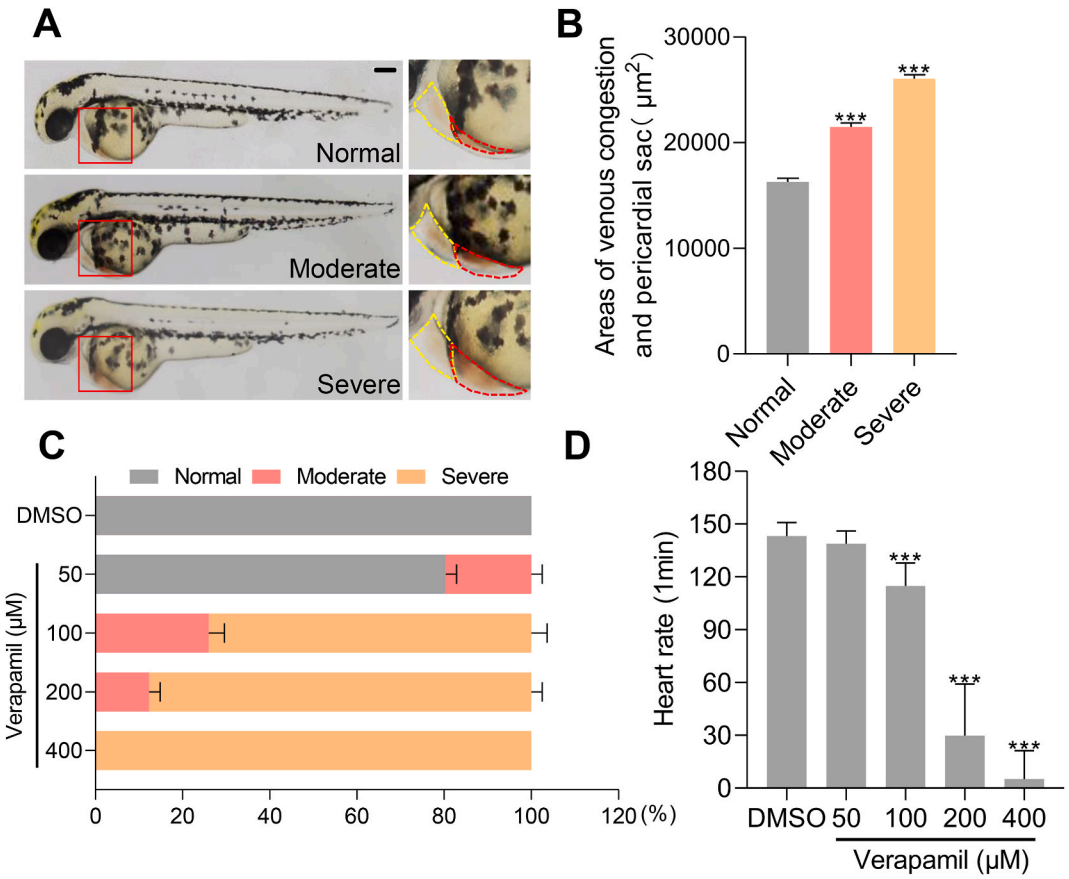

Fig. 2. Effects of verapamil on cardiac phenotype and heart rate of zebrafish embryos **A.** 52 hpf zebrafish embryos were exposed to various doses of verapamil (0–400 μM) for 30 min. The phenotypes were classified as normal, moderate and severe according to the area of the pericardial sac and venous congestion. The yellow and red-dotted lines indicate the area of the pericardial sac and venous congestion, respectively, scale bar = 200 μm. **B.** Statistics of phenotypic proportions of zebrafish embryos exposed to different doses of verapamil (0–400 μM) for 30 min, n = 30, the experiment was replicated three times. **C.** Statistics of heart rate of zebrafish embryos exposed to different doses of verapamil (0–400 μM) for 30 min, n = 30, compared with those of the 0 μM treated group (DMSO group).

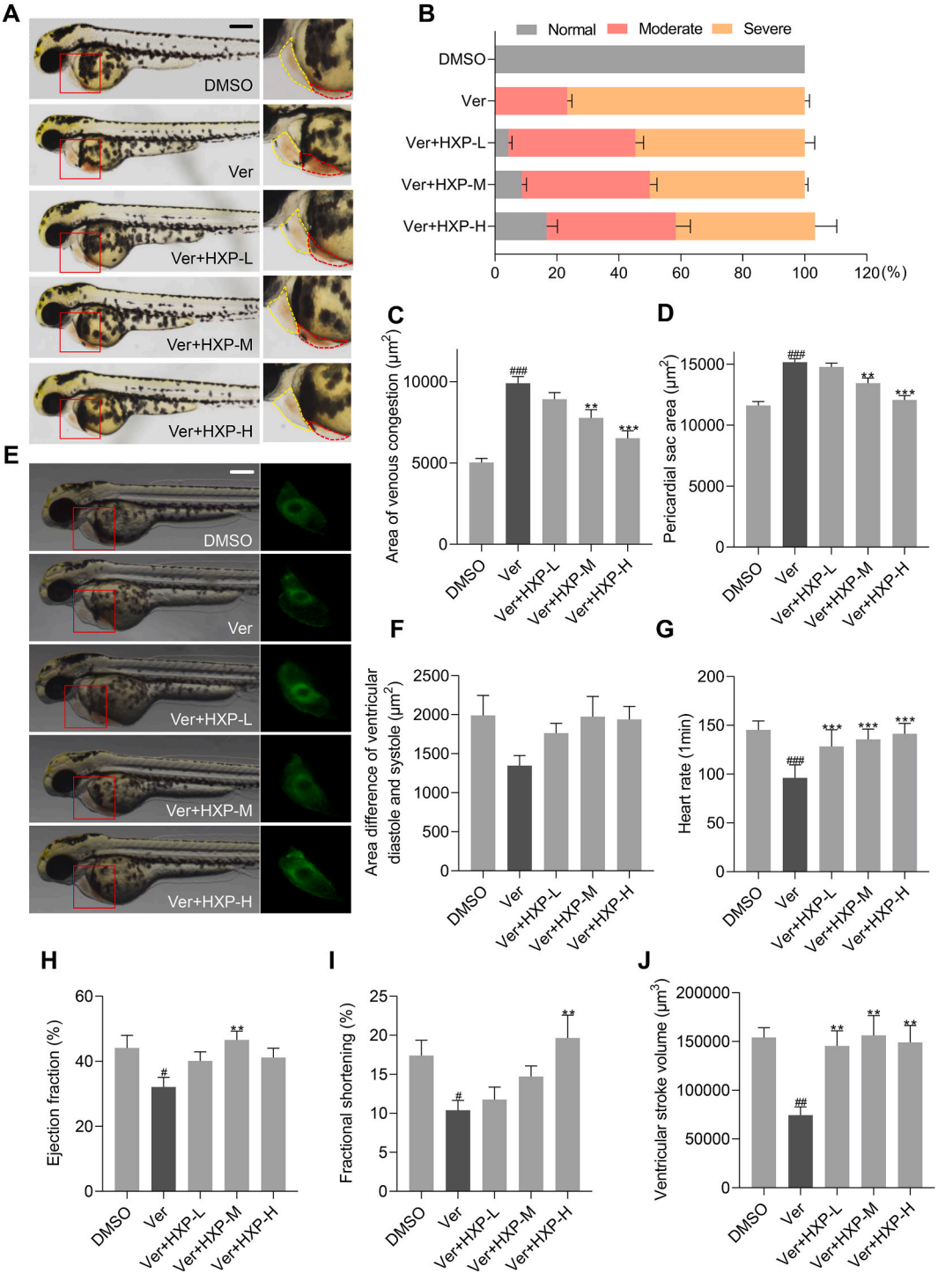

(caption on next page)

Fig. 3. HXP protects against verapamil-induced zebrafish HF in a dose-dependent manner **A.** Zebrafish embryos at 48 hpf were pretreated with low, medium or high doses of HXP for 4 h followed by exposure to 100 μM verapamil for 30 min. Representative pictures of zebrafish embryos in each group are shown. The yellow and red-dotted lines indicate the area of the pericardial sac and venous congestion, respectively, scale bar = 200 μm. **B.** The phenotypes of embryos were classified as normal, moderate and severe according to the area of the pericardial sac and venous congestion, and the phenotypic proportions of zebrafish embryos in each group were statistically analyzed, n = 30. The experiment was replicated three times. **C.** Statistics of venous congestion area of zebrafish embryos in each group, n = 10. **D.** Statistics of the pericardial sac area of zebrafish embryos in each group, n = 11. **E.** Representative pictures of zebrafish heart morphology in each group, noting that the heart was dilated in the verapamil group and that the malformation of the heart could be rescued by different doses of HXP. **F.** Statistics of the area difference of ventricular diastole and systole of zebrafish embryos in each group, n = 10. **G.** Statistics of the heart rate of zebrafish embryos in each group, n = 30. **H.** Statistics of the ejection fraction of zebrafish hearts in each group, n = 11. **I.** Statistics of fraction shortening of zebrafish hearts in each group, n = 7; **J.** Statistics of cardiac stroke volume of zebrafish embryos in each group, n = 11. $^{\#}$, $^{\#\#\#}$ Compared with the control group (DMSO group); *, **, *** compared with the verapamil group.

fraction, fractional shortening and ventricular stroke volume of the embryos were significantly reduced in the verapamil-treated group ($P < 0.05$). However, these cardiac function related parameters could be elevated to some extent when pretreated with low, medium or high concentrations of HXP (Fig. 3G–J). Genetically, verapamil induced the upregulation of key transcription factors related to zebrafish heart development, such as *nkx2.5*, *tbx5*, *gata5* and *hand2*, and their expression level could be reduced when pretreated with high concentrations of HXP (Fig. S2).

Combined with the analysis of the above data, we conclude that HXP could effectively alleviate verapamil-induced zebrafish HF,

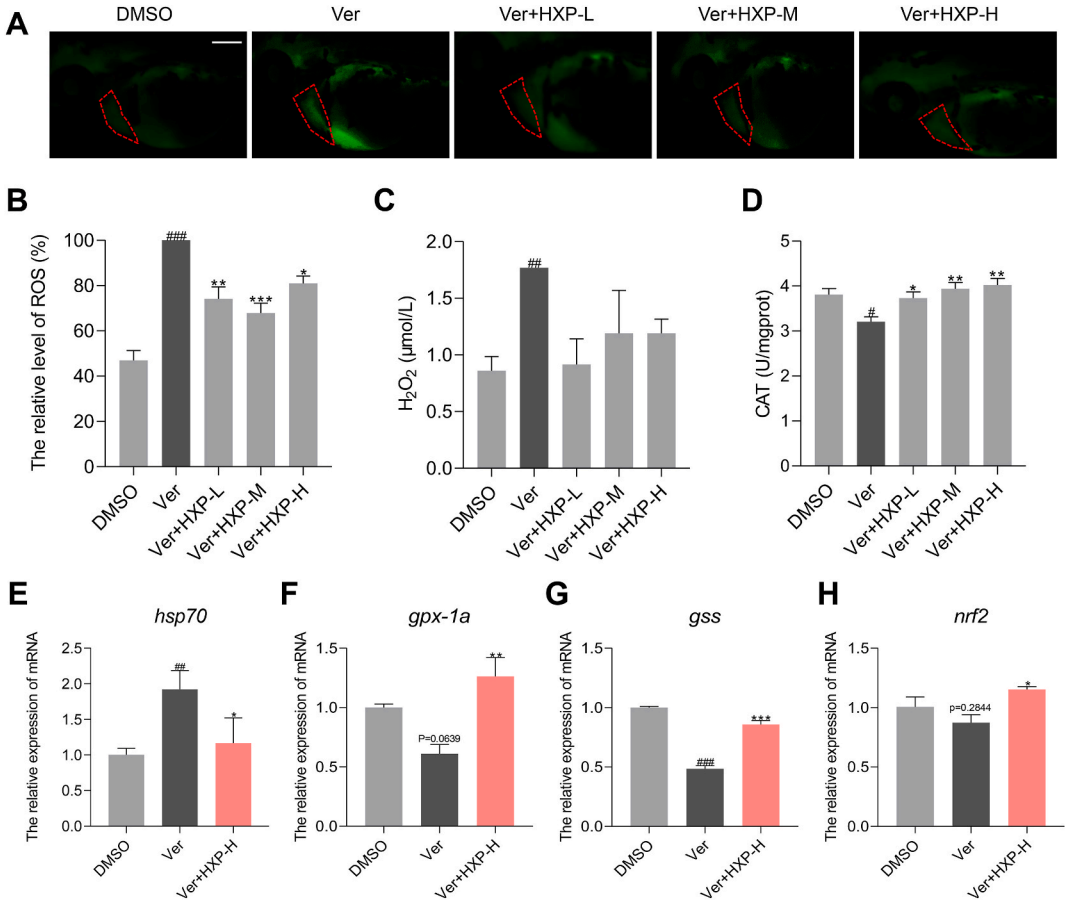

Fig. 4. HXP alleviates verapamil-induced oxidative stress in the zebrafish HF model **A.** Representative pictures of zebrafish embryos labeled with the ROS probe in each group. Red dotted lines indicate the heart area, and the fluorescence intensity represents the ROS content in the heart, scale bar = 200 μm. **B.** The relative level of ROS in zebrafish hearts of each group. The ROS level in the verapamil group was set as 100 %, n = 9. **C.** H_2O_2 content of zebrafish embryos in each group, n = 20, the experiment was replicated three times. **D.** CAT level of zebrafish embryos in each group, n = 20, the experiment was replicated three times. **E.** Relative mRNA expression of *hsp70* in zebrafish embryos in each group. **F.** Relative mRNA expression of *gpx-1a* in zebrafish embryos in each group. **G.** Relative mRNA expression of *gss* in zebrafish embryos in each group. **H.** Relative mRNA expression of *nrf2* in zebrafish embryos in each group.
$^{\#\#}$, $^{\#\#\#}$ Compared with the control group (DMSO group); *, **, *** compared with the verapamil group.

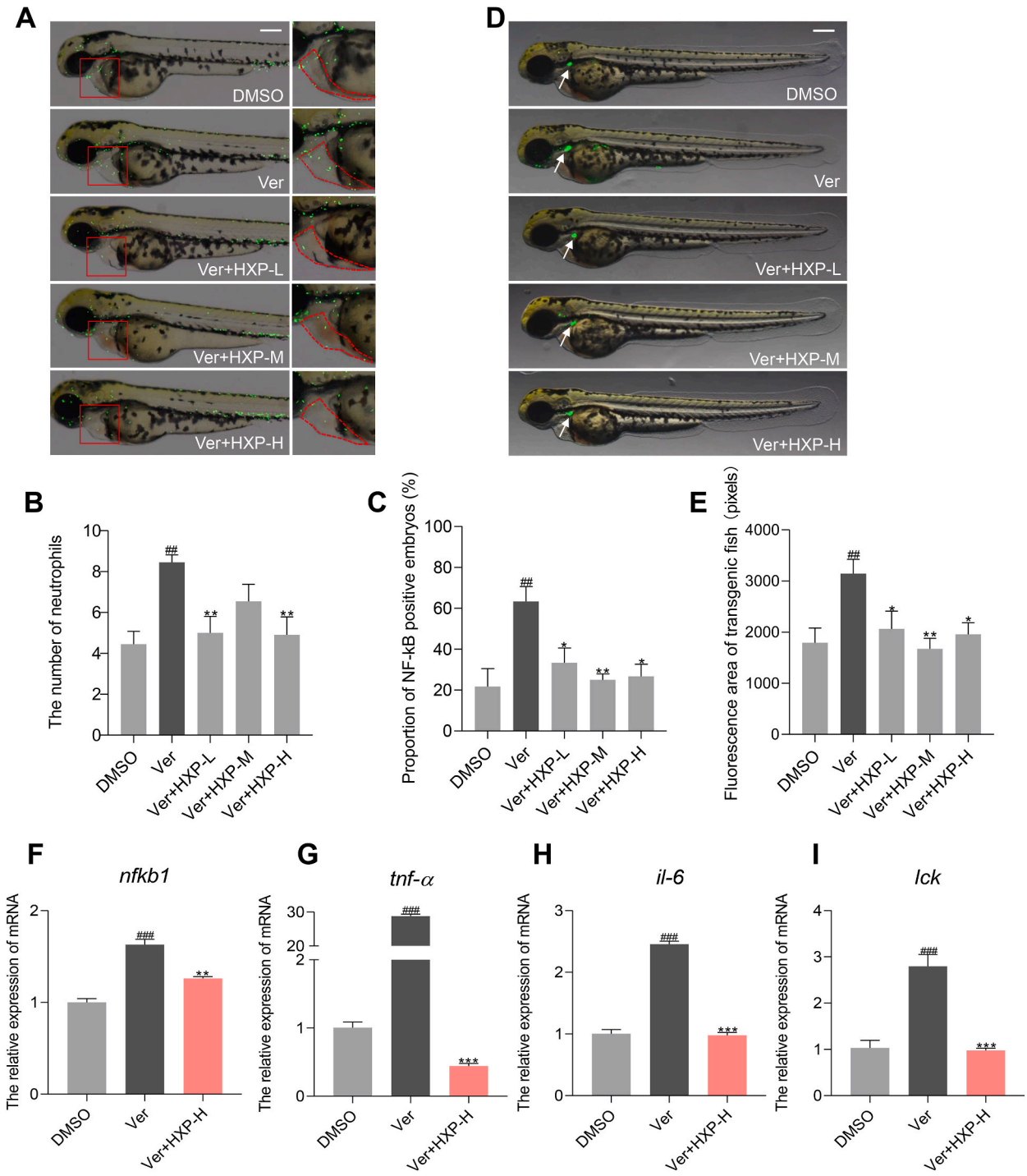

Fig. 5. HXP protects zebrafish embryos from verapamil-induced heart inflammation **A.** Representative embryos in each group showing neutrophil infiltration in hearts. Red dotted lines show the heart region, scale bar = 200 μm. **B.** Statistics of the number of neutrophils in zebrafish hearts of each group, n = 15, the experiment was replicated three times. **C.** Statistics of the proportion of NF-κB-positive embryos in each group, n = 20, the experiment was replicated three times. **D.** Representative images of NF-κB-positive embryos in each group, scale bar = 200 μm. **E.** Statistics of the fluorescence area of NF-κB-positive embryos in each group, n = 7. **F.** Relative mRNA expression of *nfkb1* in zebrafish embryos in each group. **G.** Relative mRNA expression of *tnf-α* in zebrafish embryos in each group. **H.** Relative mRNA expression of *il-6* in zebrafish embryos in each group. **I.** Relative mRNA expression of *lck* in zebrafish embryos in each group. $^{\#}$, $^{\#\#}$, $^{\#\#\#}$ Compared with the control group (DMSO group); *, **, *** compared with the verapamil group.

among which medium and high concentrations of HXP showed better protective effects.

3.4. HXP alleviates verapamil-induced oxidative stress in HF zebrafish embryos

To investigate whether HXP could alleviate verapamil-induced oxidative stress in the zebrafish HF model, we utilized a DCFH-DA probe to detect ROS levels. The fluorescence intensity in the heart region of embryos treated with verapamil increased by 53.1 % when compared with the control group ($P < 0.001$), and pretreatment with low, medium and high concentrations of HXP could decrease the ROS level by 25.9 %, 32.1 % and 19.0 %, respectively (Fig. 4A and B). Moreover, the level of H_2O_2, which is a byproduct of ROS metabolism, was obviously elevated by 110 % ($P < 0.01$) in verapamil treatment group compared to control group, and pretreatment with HXP alleviated the excessive production of H_2O_2 induced by verapamil treatment (Fig. 4C). Accordingly, the level of CAT, which is an enzyme that can decompose H_2O_2, decreased by 16 % ($P < 0.01$) in verapamil group, compared with that of control group while HXP pretreatment elevated CAT level to that of control group (Fig. 4D). At the molecular level, the expression of the stress-related gene *hsp70* was upregulated ($P < 0.01$) by verapamil treatment but inhibited by pretreatment with a high concentration of HXP (Fig. 4E). In addition, pretreatment with a high concentration of HXP elevated the expression of antioxidant genes such as *gpx-1a*, *gss* and *nrf2* (Fig. 4F–H) but not *trx* (Fig. S3) compared with that in the verapamil-induced model group.

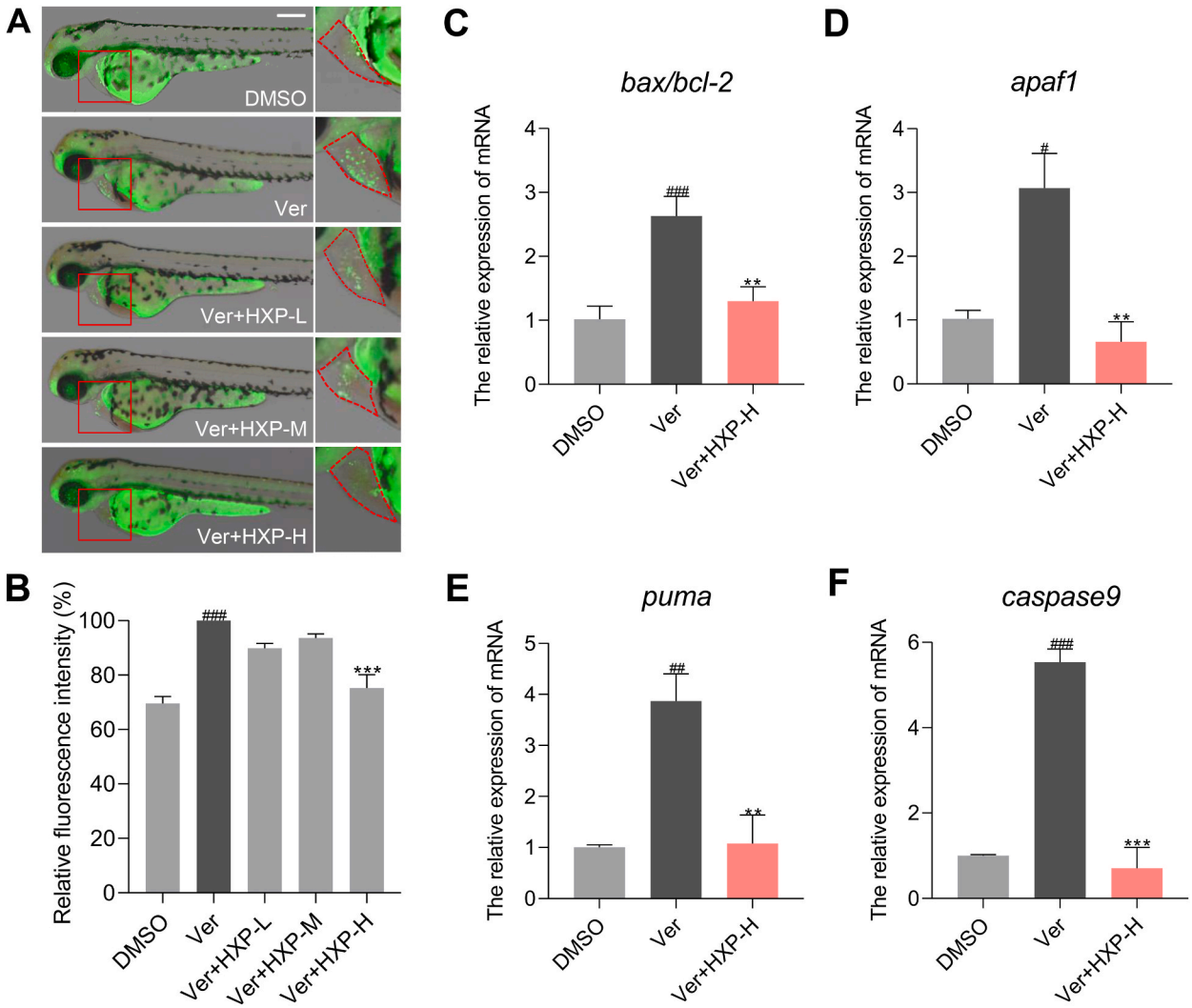

Fig. 6. HXP inhibits verapamil-induced cardiac apoptosis in zebrafish embryos **A.** Representative embryos with AO staining in each group. Red dotted lines show the heart region with apoptotic cells, scale bar = 200 μm. **B.** Relative quantification of the fluorescence intensity of zebrafish hearts in each group. The fluorescence intensity in the verapamil group was set as 100 %, n = 9. **C.** The relative mRNA expression ratio of *bax* to *bcl-2* in zebrafish embryos in each group. **D.** Relative mRNA expression of *apaf1* in zebrafish embryos in each group. **E.** Relative mRNA expression of *puma* in zebrafish embryos in each group. **F.** Relative mRNA expression of *caspase9* in zebrafish embryos in each group. $^{\#}$, $^{\#\#}$, $^{\#\#\#}$ Compared with the control group (DMSO group); *, ** compared with the verapamil group.

3.5. HXP protects zebrafish embryos from verapamil-induced heart inflammation

To investigate whether HXP could protect zebrafish embryos from verapamil-induced HF through inflammation inhibition, we administered transgenic zebrafish *Tg(mpx:EGFP),* whose neutrophils were labeled with green fluorescent protein, with HXP and verapamil, and the embryos were observed and photographed under a fluorescence microscope. The number of cardiac neutrophils was counted, and we found that it increased by 89.8 % in the verapamil group compared with the control group ($P < 0.01$). Notably, it decreased by 40.9 %, 22.6 and 41.9 % in the Ver + HXP-L, Ver + HXP-M an Ver + HXP-H groups respectively when compared with verapamil group (Fig. 5A and B). Additionally, a transgenic zebrafish *Tg(nfkb:EGFP)* was administered to assess the level of inflammation directly by fluorescence signals. The proportion of NF-kB positive embryos increased from 21.7 % to 63.3 % after verapamil induction, and the proportion decreased to 33.3 %, 25.0 % and 26.7 % when pretreated with low, medium and high concentrations of HXP respectively (Fig. 5C). Notably, the fluorescence area of NF-kB-positive embryos in the verapamil group was largely increased compared with that in the control group, while different concentrations of HXP significantly decreased the fluorescence area compared with that of the verapamil group (Fig. 5D and E).

At the molecular level, the mRNA expression of *nfkb1*, *tnf-α*, *il-6* and *lck* was detected by RT−PCR. Compared with those in the control group, the expression levels of *nfkb1*, *tnf-α*, *il-6* and *lck* were significantly increased in the verapamil group ($P < 0.01$), while their expression levels in the Ver + HXP-H group were obviously decreased compared with those in the verapamil group ($P < 0.01$) (Fig. 5F–I).

3.6. HXP inhibits verapamil-induced cell apoptosis in zebrafish embryos

AO staining was conducted to detect cell apoptosis in zebrafish embryos treated with verapamil alone or pretreated with different concentrations of HXP. The representative images showed that the embryos in the verapamil group showed much more densely stained yellow green fluorescence with yellow green debris particles in the heart region than those in the control group. Compared with the verapamil group, the fluorescence intensity in the heart region was overtly decreased in the Ver + HXP-L, Ver + HXP-M and Ver + HXP-H groups (Fig. 6A). Accordingly, statistical analysis of the images showed that the fluorescence intensity of the heart region in the verapamil group was significantly elevated compared with that in the control group ($P < 0.001$). However, the cardiac fluorescence intensity in the Ver + HXP-L, Ver + HXP-M and Ver + HXP-H groups was dramatically decreased (Fig. 6B). This indicated that verapamil induced cell apoptosis in zebrafish hearts, while HXP alleviated verapamil induced cell apoptosis in zebrafish hearts.

Furthermore, the gene expression levels of key factors involved in cell apoptosis, such as *bax*, *bcl-2*, *apaf1*, *puma* and *caspase-9,* were detected by RT−PCR. First, the expression ratio of *bax/bcl-2*, which indicates cell apoptosis, was significantly upregulated in the verapamil group, and the elevation was strongly inhibited by pretreatment with a high concentration of HXP (Fig. 6C). Second, the expression of *apaf1* in the verapamil group was largely increased compared with that in the control group ($P < 0.05$), while its upregulation could be robustly inhibited in the Ver + HXP-H group ($P < 0.05$) (Fig. 6D). Third, the expression of *puma*, an inducer of cell apoptosis, was also significantly increased in the verapamil group compared with the control group ($P < 0.01$). However, in the Ver + HXP-H group, its mRNA expression level was reduced to that in the control group ($P < 0.01$) (Fig. 6E). Finally, the expression of *caspase-9*, an upstream inducer of apoptosis, was significantly increased in the verapamil group compared with the control group ($P < 0.001$). Its expression was significantly decreased in the Ver + HXP-H group ($P < 0.001$) (Fig. 6F). These data suggest that the high concentration of HXP exhibits a strong protective effect on verapamil induced cardiac apoptosis in zebrafish embryos.

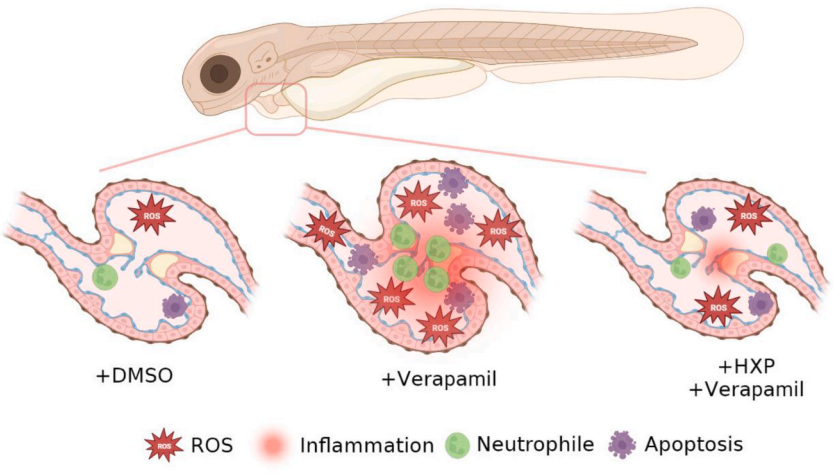

Fig. 7. Diagram illustrating the mechanism by which HXP alleviates verapamil-induced HF in zebrafish embryos.

4. Discussion

Heart failure is the terminal pathological event of several cardiac diseases, including myocardial infarction, cardiac hypertrophy and hypertension [37]. Increased generation of ROS followed by inflammation and apoptosis is implicated in the pathogenesis of HF. Our results indicate that HXP, a traditional Chinese herbal medicine, can effectively strengthen cardiac function through the ROS mediated NF-κB pathway, resulting in attenuation of inflammation and apoptosis in the context of a verapamil-induced zebrafish HF model. Fig. 7 illustrated the molecular mechanism through which HXP alleviates verapamil-induced heart failure in zebrafish embryos.

The zebrafish has become an important model in life science for its unique advantages in imaging and genetic manipulation and has helped identify new genes, modifiers and drugs [38–40]. Not only drug-induced but also genetic and other kinds of HF models could be generated in zebrafish [41]. In this study, *Tg(mpx:EGFP)* and *Tg(nfkb:EGFP)* transgenic lines were used to assess the level of inflammation by directly observing neutrophil infiltration and the expression of NF-kB, and the *Tg(myl7:EGFP)* line was used to enable nonintrusive visualization of the heart in vivo in the pathogenesis of HF. Prior studies indicated that the verapamil (200 μM)-induced larval zebrafish HF model is a useful tool for whole animal HF studies and for screening safe agents of HF [20,42]. Our results found that zebrafish treated with 100 μM verapamil exhibited obvious HF phenotypes and weakened cardiac function. The different verapamil concentrations may result from the different drug sources and batches. These data indicated that the HF zebrafish model was successfully established and can be utilized as an alternative, novel and simple experimental animal model of heart failure.

Clinically, HXP has been utilized for the treatment of coronary heart disease for more than 40 years with favorable therapeutic effects. There are many important active compounds in Huoxin pills, which have antioxidant, anti-inflammatory and anti-apoptotic effects. For example, network pharmacological analysis and experiments have proven that quercetin and kaempferol have anti-inflammatory and anti-apoptotic effects [9], and ginsenoside has been proven to have antioxidant effects [43]. The abnormal cardiac phenotypes in zebrafish larva induced by verapamil, can be rescued by HXP administration, whereas not all the fish in the prevention group were able to completely recover after verapamil treatment. This could be partly attributed to the muscone from the *Moschus* component in HXP, which had toxic effects on zebrafish embryos [5]. Therefore, further optimization of the Chinese herbal formula of HXP may be able to obtain a better therapeutic effect on HF. And in this study, we did not dissect the hearts from the small zebrafish larvae to examine the cellular and molecular indicators, therefore, much more elaborate experiments including micro and single cell analysis should be done to further prove our findings.

A basal concentration of ROS is essential for the manifestation of normal cellular functions, while excessive levels of ROS cause damage to tissue, eventually leading to inflammation and apoptosis [44]. HXP has been proven to prevent H_2O_2-induced DNA damage in AC16 cardiomyocytes [45]. In vivo, we demonstrated that HXP could significantly inhibit excessive production of ROS in the hearts as well as H_2O_2 levels in HF zebrafish larvae, and enhanced the CAT activity of HF zebrafish. These findings suggest that HXP may have a cardioprotective effect by suppressing excessive oxidative stress. Mechanistically, HXP upregulated the expression of antioxidant genes, including *gpx-1a*, *gss* and *nrf2,* but not *trx*, suggesting that it may exert its efficacy mainly by regulating the glutathione peroxidase system and Nrf2 antioxidant system but not the thioredoxin antioxidant system. It is well established that ROS and inflammation are closely intertwined [46]. ROS accumulation induced by oxidative stress activates the inflammatory signaling pathway, which in turn accelerates ROS generation and aggravates oxidative stress. Neutrophils, the most abundant leukocytes, are known to be the first cells to reach the site of inflammation and play an essential role in the inflammatory response [47]. Here, we found that HXP improves cardiac function by reducing neutrophil infiltration and downregulating *tnf-α* and *il-6* transcriptional levels induced by verapamil in larval zebrafish. However, whether *tnf-α* and *il-6* are primarily derived from neutrophils is unknown, and the pathway by which HXP affects neutrophils still warrants future investigation.

ROS have been implicated in the signaling pathway leading to NF-κB activation, which is sufficient for inflammatory activation [48,49]. In addition, the transcription factor NF-κB is central to guiding neutrophil activation and extending the neutrophil life span [50]. In line with the alteration of neutrophil infiltration, we found that the transcriptional levels of *nfkb1* were evidently reduced with HXP administration compared with the model group. Additionally, a transgenic line *Tg(nfkb:EGFP)* was administered for inflammation evaluation, and we found that HXP could inhibit the activation of NF-kB expression induced by verapamil. In addition, ROS are known to promote apoptosis, which has significant pathophysiological consequences that lead to abnormalities in the myocardium. Bcl-2 family proteins are the key regulators of apoptosis, and the ratio of Bax/Bcl-2 in cardiomyocytes determines whether they will survive or die [51]. In the present study, we demonstrated that HXP could inhibit apoptosis by reducing the number of apoptotic cells and dramatically downregulating the expression ratio of *bax/bcl-2* and the mRNA expression levels of *apaf1*, *puma* and *caspase9*. We speculate that HXP predominantly suppresses the ROS-induced NF-κB signaling pathway, thereby exerting its antiapoptotic effects that protect the heart against oxidative stress. Further studies are needed to explore how HXP suppresses the production of ROS to protect cardiac function.

These genes/biochemical assays are not specific to the heart except the general phenotype, ROS, neutrophils and NF-κB assays. To exclude the general toxic response of HXP on zebrafish heart development and function, two statements were clarified here. First, we have test the toxic effect of HXP on healthy embryos and found that the concentrations below 20 μg/mL will not cause any development toxicity. However, when HF zebrafish were treated with 20 μg/mL HXP, the heart function can be improved and the HF phenotypes can be reduced significantly. This comparative analysis provides an evidence that HXP's effects are specific to HF. Additionally, different concentrations of HXP have been administrated to test the dose-dependent effects on HF zebrafish, and we found that higher concentrations of the drug leading to more pronounced improvements in heart function. This supports the notion that HXP is targeting the underlying pathological processes of zebrafish HF rather than causing non-specific toxicity.

Overall, our study utilized a verapamil-induced zebrafish HF model to explore the molecular mechanism involved in the therapeutic effect of HXP. We propose that HXP protects against HF mainly via regulation of the ROS-induced NF-κB signaling pathway,

which could induce neutrophil infiltration, proinflammatory cytokine secretion and cell apoptosis. Our findings, along with data showing the good efficacy of HXP in mice and rats [7,9,52], lay a primary foundation to investigate the molecular mechanism of HXP in improving cardiac function.

5. Conclusion

The current study explored the therapeutic effect of HXP on HF in a verapamil-induced zebrafish HF model. The findings show that HXP could alleviate verapamil-induced HF via improving cardiac function, such as by elevating heart rate and reducing venous congestion. In terms of mechanism, HXP protects against zebrafish HF through inhibiting levels of heart oxidative stress, inflammation and apoptosis, mainly via regulation of the ROS-induced NF-κB signaling pathway. Our study provides scientific evidence by which HXP could be used to treat HF, and the clinical application of HXP for many other cardiovascular diseases could be considered in the future.

Funding

This research was funded by the Fujian Provincial Natural Science Foundation (2021J05063), China ; Scientific Research Foundation for the High-level Talents, Fujian University of Traditional Chinese Medicine (X2021007-talents) , China; Fujian University of Traditional Chinese Medicine Foundation (X2021017-Key), China.

Data availability statement

Data will be made available on request.

CRediT authorship contribution statement

Xianmei Li: Writing – review & editing, Supervision, Project administration, Funding acquisition, Conceptualization. **Laifeng Zeng:** Writing – original draft, Methodology, Investigation, Formal analysis, Data curation. **Zhixin Qu:** Resources, Methodology, Investigation. **Fenghua Zhang:** Writing – review & editing, Writing – original draft, Supervision, Resources, Formal analysis, Conceptualization.

Declaration of competing interest

The authors declare that they have no known competing financial interests or personal relationships that could have appeared to influence the work reported in this paper.

Acknowledgments

We thank Fuzhou Bioservice Biotechnology Co., Ltd. for offering the *Tg(nfkb:EGFP)* transgenic line and zebrafish rearing.

Abbreviations

HF	heart failure
HXP	Huoxin Pill
TCM	traditional Chinese medicine
ROS	reactive oxygen species
NF-κB	nuclear factor κB
NOAEL	no observed adverse effect level
hpf	hours post fertilization

Appendix A. Supplementary data

Supplementary data to this article can be found online at https://doi.org/10.1016/j.heliyon.2023.e23402.

References

[1] G. Savarese, L.H. Lund, Global public health burden of heart failure, Card. Fail. Rev. 3 (2017) 7–11, https://doi.org/10.15420/cfr.2016:25:2.
[2] L.H. Lund, J.J. Carrero, B. Farahmand, K.M. Henriksson, A. Jonsson, T. Jernberg, et al., Association between enrolment in a heart failure quality registry and subsequent mortality-a nationwide cohort study, Eur. J. Heart Fail. 19 (2017) 1107–1116, https://doi.org/10.1002/ejhf.762.

[3] T. Thorvaldsen, L. Benson, U. Dahlstrom, M. Edner, L.H. Lund, Use of evidence-based therapy and survival in heart failure in Sweden 2003-2012, Eur. J. Heart Fail. 18 (2016) 503–511, https://doi.org/10.1002/ejhf.496.

[4] C.S. Weldy, E.A. Ashley, Towards precision medicine in heart failure, Nat. Rev. Cardiol. 18 (2021) 745–762, https://doi.org/10.1038/s41569-021-00566-9.

[5] Q. Zhang, D. Guo, Y. Wang, X. Wang, Q. Wang, Y. Wu, et al., Danqi pill protects against heart failure post-acute myocardial infarction via HIF-1alpha/PGC-1alpha mediated glucose metabolism pathway, Front. Pharmacol. 11 (2020) 458, https://doi.org/10.3389/fphar.2020.00458.

[6] Y. Zhao, Y. Li, L. Tong, X. Liang, H. Zhang, L. Li, et al., Analysis of microRNA expression profiles induced by Yiqifumai injection in rats with chronic heart failure, Front. Physiol. 9 (2018) 48, https://doi.org/10.3389/fphys.2018.00048.

[7] M.Z. Peng, M.L. Yang, A.L. Shen, X.L. Zhou, Y. Lu, Q. Li, et al., Huoxin pill attenuates cardiac fibrosis by suppressing TGF-β1/smad2/3 pathway in isoproterenol-induced heart failure rats, Chin. J. Integr. Med. 27 (2021) 424–431, https://doi.org/10.1007/s11655-020-2862-8.

[8] Y. Xu, H. Hu, Y. Li, R. Cen, C. Yao, W. Ma, et al., Effects of huoxin formula on the arterial functions of patients with coronary heart disease, Pharm. Biol. 57 (2019) 13–20, https://doi.org/10.1080/13880209.2018.1561726.

[9] J. He, D. Wo, E. Ma, Q. Wang, J. Chen, J. Peng, et al., Network pharmacology-based analysis in determining the mechanisms of Huoxin pill in protecting against myocardial infarction, Pharmaceut. Biol. 59 (2021) 1191–1202, https://doi.org/10.1080/13880209.2021.1964542.

[10] J. Meng, B. Yang, Protective effect of Ganoderma (lingzhi) on cardiovascular system, Adv. Exp. Med. Biol. 1182 (2019) 181–199, https://doi.org/10.1007/978-981-32-9421-9_7.

[11] C.H. Lee, J.H. Kim, A review on the medicinal potentials of ginseng and ginsenosides on cardiovascular diseases, J Ginseng Res 38 (2014) 161–166, https://doi.org/10.1016/j.jgr.2014.03.001.

[12] G. Bowley, E. Kugler, R. Wilkinson, A. Lawrie, F. van Eeden, Chico Tja, et al., Zebrafish as a tractable model of human cardiovascular disease, Br. J. Pharmacol. 179 (2022) 900–917, https://doi.org/10.1111/bph.15473.

[13] P. Novodvorsky, M.M. Da Costa, T.J. Chico, Zebrafish-based small molecule screens for novel cardiovascular drugs, Drug Discov. Today Technol. 10 (2013) e109–e114, https://doi.org/10.1016/j.ddtec.2012.01.005.

[14] K. Howe, M.D. Clark, C.F. Torroja, J. Torrance, C. Berthelot, M. Muffato, et al., The zebrafish reference genome sequence and its relationship to the human genome, Nature 496 (2013) 498–503, https://doi.org/10.1038/nature12111.

[15] M.H. Lin, H.C. Chou, Y.F. Chen, W. Liu, C.C. Lee, L.Y. Liu, et al., Development of a rapid and economic in vivo electrocardiogram platform for cardiovascular drug assay and electrophysiology research in adult zebrafish, Sci. Rep. 8 (2018), 15986, https://doi.org/10.1038/s41598-018-33577-7.

[16] D. Staudt, D. Stainier, Uncovering the molecular and cellular mechanisms of heart development using the zebrafish, Annu. Rev. Genet. 46 (2012) 397–418, https://doi.org/10.1146/annurev-genet-110711-155646.

[17] D. Ling, H. Chen, G. Chan, S.M. Lee, Quantitative measurements of zebrafish heartrate and heart rate variability: a survey between 1990-2020, Comput. Biol. Med. 142 (2022), 105045, https://doi.org/10.1016/j.compbiomed.2021.105045.

[18] C.C. Huang, A. Monte, J.M. Cook, M.S. Kabir, K.P. Peterson, Zebrafish heart failure models for the evaluation of chemical probes and drugs, Assay Drug Dev. Technol. 11 (2013) 561–572, https://doi.org/10.1089/adt.2013.548.

[19] X. Shi, S. Verma, J. Yun, K. Brand-Arzamendi, K.K. Singh, X. Liu, et al., Effect of empagliflozin on cardiac biomarkers in a zebrafish model of heart failure: clues to the EMPA-REG OUTCOME trial? Mol. Cell. Biochem. 433 (2017) 97–102, https://doi.org/10.1007/s11010-017-3018-9.

[20] X.Y. Zhu, S.Q. Wu, S.Y. Guo, H. Yang, B. Xia, P. Li, et al., A zebrafish heart failure model for assessing therapeutic agents, Zebrafish 15 (2018) 243–253, https://doi.org/10.1089/zeb.2017.1546.

[21] S.H. Shin, S. Lee, J.S. Bae, J.G. Jee, H.J. Cha, Y.M. Lee, Thymosin beta4 regulates cardiac valve formation via endothelial-mesenchymal transformation in zebrafish embryos, Mol. Cell. 37 (2014) 330–336, https://doi.org/10.14348/molcells.2014.0003.

[22] R. Dong, Y. Zhang, S. Chen, H. Wang, K. Hu, H. Zhao, et al., Identification of key pharmacodynamic markers of American ginseng against heart failure based on metabolomics and zebrafish model, Front. Pharmacol. 13 (2022), 909084, https://doi.org/10.3389/fphar.2022.909084.

[23] S. Li, H. Liu, Y. Li, X. Qin, M. Li, J. Shang, et al., Shen-yuan-dan capsule attenuates verapamil-induced zebrafish heart failure and exerts antiapoptotic and anti-inflammatory effects via reactive oxygen species-induced NF-κB pathway, Front. Pharmacol. 12 (2021), 626515, https://doi.org/10.3389/fphar.2021.626515.

[24] X. Guo, M. Dumas, B.L. Robinson, S.F. Ali, M.G. Paule, Q. Gu, et al., Acetyl L-carnitine targets adenosine triphosphate synthase in protecting zebrafish embryos from toxicities induced by verapamil and ketamine: an in vivo assessment, J. Appl. Toxicol. : JAT 37 (2017) 192–200, https://doi.org/10.1002/jat.3340.

[25] M.F. Hill, P.K. Singal, Right and left myocardial antioxidant responses during heart failure subsequent to myocardial infarction, Circulation 96 (1997) 2414–2420, https://doi.org/10.1161/01.cir.96.7.2414.

[26] Z. Mallat, I. Philip, M. Lebret, D. Chatel, J. Maclouf, A. Tedgui, Elevated levels of 8-iso-prostaglandin F2alpha in pericardial fluid of patients with heart failure: a potential role for in vivo oxidant stress in ventricular dilatation and progression to heart failure, Circulation 97 (1998) 1536–1539, https://doi.org/10.1161/01.cir.97.16.1536.

[27] P. Korantzopoulos, T. Kolettis, K. Siogas, J. Goudevenos, Atrial fibrillation and electrical remodeling: the potential role of inflammation and oxidative stress, Med. Sci. Mon. Int. Med. J. Exp. Clin. Res. 9 (2003) RA225–R229.

[28] M.D. Engelmann, J.H. Svendsen, Inflammation in the genesis and perpetuation of atrial fibrillation, Eur. Heart J. 26 (2005) 2083–2092, https://doi.org/10.1093/eurheartj/ehi350.

[29] A. Kumar, S. Supowit, J.D. Potts, D.J. DiPette, Alpha-calcitonin gene-related peptide prevents pressure-overload induced heart failure: role of apoptosis and oxidative stress, Phys. Rep. 7 (2019), e14269, https://doi.org/10.14814/phy2.14269.

[30] M. Wang, Y. Tan, Y. Shi, X. Wang, Z. Liao, P. Wei, Diabetes and sarcopenic obesity: pathogenesis, diagnosis, and treatments, Front. Endocrinol. 11 (2020) 568, https://doi.org/10.3389/fendo.2020.00568.

[31] X. Liu, B. Lu, J. Fu, X. Zhu, E. Song, Y. Song, Amorphous silica nanoparticles induce inflammation via activation of NLRP3 inflammasome and HMGB1/TLR4/MYD88/NF-kb signaling pathway in HUVEC cells, J. Hazard Mater. 404 (2021), 124050, https://doi.org/10.1016/j.jhazmat.2020.124050.

[32] M. Dutka, R. Bobinski, I. Ulman-Wlodarz, M. Hajduga, J. Bujok, C. Pajak, et al., Various aspects of inflammation in heart failure, Heart Fail. Rev. 25 (2020) 537–548, https://doi.org/10.1007/s10741-019-09875-1.

[33] L. Dewachter, C. Dewachter, Inflammation in right ventricular failure: does it matter? Front. Physiol. 9 (2018) 1056, https://doi.org/10.3389/fphys.2018.01056.

[34] L. Laugier, L.R.P. Ferreira, F.M. Ferreira, S. Cabantous, A.F. Frade, J.P. Nunes, et al., miRNAs may play a major role in the control of gene expression in key pathobiological processes in Chagas disease cardiomyopathy, PLoS Neglected Trop. Dis. 14 (2020), e0008889, https://doi.org/10.1371/journal.pntd.0008889.

[35] C.B. Kimmel, W.W. Ballard, S.R. Kimmel, B. Ullmann, T.F. Schilling, Stages of Embryonic Development of the Zebrafish. Developmental Dynamics, 203, an official publication of the American Association of Anatomists, 1995, pp. 253–310, https://doi.org/10.1002/aja.1002030302.

[36] C.A. Schneider, W.S. Rasband, K.W. Eliceiri, NIH Image to ImageJ: 25 years of image analysis, Nat. Methods 9 (2012) 671–675, https://doi.org/10.1038/nmeth.2089.

[37] B. Duygu, E.M. Poels, P.A. da Costa Martins, Genetics and epigenetics of arrhythmia and heart failure, Front. Genet. 4 (2013) 219, https://doi.org/10.3389/fgene.2013.00219.

[38] P. Huang, Z. Zhu, S. Lin, B. Zhang, Reverse genetic approaches in zebrafish, J Genet Genomics 39 (2012) 421–433, https://doi.org/10.1016/j.jgg.2012.07.004.

[39] A. Asnani, R.T. Peterson, The zebrafish as a tool to identify novel therapies for human cardiovascular disease, Dis Model Mech 7 (2014) 763–767, https://doi.org/10.1242/dmm.016170.

[40] L.I. Zon, R.T. Peterson, In vivo drug discovery in the zebrafish, Nat. Rev. Drug Discov. 4 (2005) 35–44, https://doi.org/10.1038/nrd1606.

[41] S. Narumanchi, H. Wang, S. Perttunen, I. Tikkanen, P. Lakkisto, J. Paavola, Zebrafish heart failure models, Front. Cell Dev. Biol. 9 (2021), 662583, https://doi.org/10.3389/fcell.2021.662583.

[42] J. Liu, Y. Liu, H. Yu, Y. Zhang, A.C. Hsu, M. Zhang, et al., Design, synthesis and biological evaluation of novel pyxinol derivatives with anti-heart failure activity, Biomed. Pharmacother. 133 (2021), 111050, https://doi.org/10.1016/j.biopha.2020.111050.

[43] I.H. Baik, K.H. Kim, K.A. Lee, Antioxidant, anti-inflammatory and antithrombotic effects of ginsenoside compound K enriched extract derived from ginseng sprouts, Molecules 26 (2021), https://doi.org/10.3390/molecules26134102.
[44] H. Sies, V.V. Belousov, N.S. Chandel, M.J. Davies, D.P. Jones, G.E. Mann, et al., Defining roles of specific reactive oxygen species (ROS) in cell biology and physiology, Nat. Rev. Mol. Cell Biol. 23 (2022) 499–515, https://doi.org/10.1038/s41580-022-00456-z.
[45] Q. Wang, E. Ma, D. Wo, J. Chen, J. He, J. Peng, et al., Huoxin pill prevents acute myocardial ischaemia injury via inhibition of Wnt/β-catenin signaling, J. Cell Mol. Med. 25 (2021) 11053–11062, https://doi.org/10.1111/jcmm.17028.
[46] T. Senoner, W. Dichtl, Oxidative stress in cardiovascular diseases: still a therapeutic target? Nutrients 11 (2019) https://doi.org/10.3390/nu11092090.
[47] R. Medzhitov, Inflammation 2010: new adventures of an old flame, Cell 140 (2010) 771–776, https://doi.org/10.1016/j.cell.2010.03.006.
[48] C. Bubici, S. Papa, K. Dean, G. Franzoso, Mutual cross-talk between reactive oxygen species and nuclear factor-kappa B: molecular basis and biological significance, Oncogene 25 (2006) 6731–6748, https://doi.org/10.1038/sj.onc.1209936.
[49] A. Denk, M. Goebeler, S. Schmid, I. Berberich, O. Ritz, D. Lindemann, et al., Activation of NF-kappa B via the Ikappa B kinase complex is both essential and sufficient for proinflammatory gene expression in primary endothelial cells, J. Biol. Chem. 276 (2001) 28451–28458, https://doi.org/10.1074/jbc.M102698200.
[50] P.P. McDonald, A. Bald, M.A. Cassatella, Activation of the NF-kappaB pathway by inflammatory stimuli in human neutrophils, Blood 89 (1997) 3421–3433.
[51] D.M. Valks, T.J. Kemp, A. Clerk, Regulation of Bcl-xL expression by H2O2 in cardiac myocytes, J. Biol. Chem. 278 (2003) 25542–25547, https://doi.org/10.1074/jbc.M303760200.
[52] M. Peng, M. Yang, Y. Lu, S. Lin, H. Gao, L. Xie, et al., Huoxin Pill inhibits isoproterenol-induced transdifferentiation and collagen synthesis in cardiac fibroblasts through the TGF-β/Smads pathway, J. Ethnopharmacol. 275 (2021), 114061, https://doi.org/10.1016/j.jep.2021.114061.